SANDIA REPORT

SAND2007-6205

Thermodynamics Resource Data base

M. D. Allendorf and M. Medlin
Sandia National Laboratories
Livermore, CA 94551-0969
(925) 294-2895
email: mdallen@sandia.gov

T. M. Besmann
Oak Ridge National Laboratory
PO Box 2008 MS 6063
Oak Ridge TN 37831-6063
(865)574-6852
email: tmb@ornl.gov

B&R NUMBER: ED1904032
Project period 10/2001 - 9/2006

Prepared by
Sandia National Laboratories
Albuquerque, New Mexico 87185 and Livermore, California 94550

Sandia is a multiprogram laboratory operated by Sandia Corporation,
a Lockheed Martin Company, for the United States Department of Energy's
National Nuclear Security Administration under Contract DE-AC04-94AL85000.

Issued by Sandia National Laboratories, operated for the United States Department of Energy by Sandia Corporation.

Available to DOE and DOE contractors from
U.S. Department of Energy
Office of Scientific and Technical Information
P.O. Box 62
Oak Ridge, TN 37831

Telephone: (865) 576-8401
Facsimile: (865) 576-5728
E-Mail: reports@adonis.osti.gov
Online ordering: http://www.osti.gov/bridge

Available to the public from
U.S. Department of Commerce
National Technical Information Service
5285 Port Royal Rd.
Springfield, VA 22161

Telephone: (800) 553-6847
Facsimile: (703) 605-6900
E-Mail: orders@ntis.fedworld.gov
Online order: http://www.ntis.gov/help/ordermethods.asp?loc=7-4-0#online

Acknowledgement

This work is based upon work supported by the U. S. Department of Energy under the Industrial Technology for Future Programs Office.

Disclaimer

Any findings opinions and conclusions or recommendations expressed in this report are those of the author(s) and do not necessarily reflect the view of the Department of Energy.

Proprietary Data Notice

If there is any patentable material or protected data in the report, the recipient, consistent with the data protection provisions for the award, must mark the appropriate block in Section K of the DOE F241.3 clearly specify it here, and identify them on appropriate pages of the report. Other than patentable material or protected data, reports must not contain any proprietary data (limited rights data), classified information, information subject to export control classification or other information not subject to release. Protected data is specific technical data, first produced in the performance of the award, which is protected from public release for a period of time by the terms of the award agreement. Reports delivered without such notice may be deemed to have been furnished with unlimited rights and the Government assumes no liability for the disclosure, reproduction or use of such reports.

Table of Contents

Figures

Tables

1.0 EXECUTIVE SUMMARY

Thermodynamic data, including heats of formation, heat capacities, enthalpies, and entropies, are essential for modeling high-temperature processes such as corrosion, combustion, metals processing, glass making, and chemical manufacturing and refining. Standard compilations often lack data for systems of industrial interest. In particular, oxide systems in which low-melting liquids or glasses can form, and vapor-phase systems involving compounds below the first row of the periodic table (for example, aluminum and silicon) or transition metals, are difficult to model for this reason. Since there are few experimental efforts ongoing today that can provide such data, this represents a major impediment to developing models that can be used to improve the energy efficiency of such processes and reduce waste. Fortunately, computational methods developed over the past two decades have reached a level of accuracy that can provide reliable data for many systems of interest.

The objective of this project is to provide missing thermodynamic data relevant to high-temperature industrial processes, including thermochemistry for condensed-phase systems, in particular oxides and glasses, and gas-phase data for molecules containing both main-group and transition-metal elements. Modeling approaches are used to generate the data. In particular, the Bond Additivity Correction (BAC) method and other approaches based on quantum chemistry are used to compute thermochemistry for gas-phase species. For condensed-phase systems, the Associate Species Model is applied, which has been shown to be an accurate method for generating data for the non-ideal solution phases represented by oxides and glasses. To make these data as widely accessible as possible, a web site was created where users can download any of the data obtained during the project.

http://www.ca.sandia.gov/HiTempThermo

The web site provides full documentation, including published references where available, and additional information about gas-phase species in the data base, such as structures, vibrational frequencies, and moments of inertia that are useful for modeling chemical reactions.

The data base includes thermochemistry for more than 1017 gas-phase species. Compounds of the following elements represented are included: H, Li, Be, B, C, N, O, F, Na, Mg, Al, Si, Cl, K, Ca, Cr, Mn, Fe, In, Sn, Sb. Data for a wide range of condensed-phase oxide systems are also available, including 10 different models corresponding to important refractory and corrosion systems such as alumina, mullite, calcia, silica, and chromia. All data are free.

2.0 INTRODUCTION

2.1 Project Motivation

It is not an exaggeration to say that thermodynamic property data (heats of formation, heat capacities, and entropies for both condensed- and gas-phase compounds) are the foundation of building accurate models for understanding all high-temperature processes. Such data have many uses, among them:

- equilibrium calculations to predict corrosion of refractories and other materials
- heat-transfer modeling of furnaces and molten phases of glasses and metals
- modeling of high-temperature chemical reactions occurring in material synthesis
- prediction of process energy efficiency and pollutant formation for combustion and other high-temperature manufacturing processes
- prediction of liquidus temperatures and the formation of crystalline inclusions in glass formulations

Clearly, without thermodynamic data, it would be difficult or impossible to even begin to model many high-temperature processes.

The technology roadmaps developed by various DOE-ITP Industry of the Future (IOF) working groups describe many high-priority technology barriers and research needs that in some way require detailed knowledge of materials thermochemistry. The sections below briefly describe examples of high-priority items; many lower-priority issues involving thermochemistry can be found in the IOF reports as well.

Aluminum refining: The *Material Technologies for the Process Industries of the Future*[1] report and the *Aluminum Industry Technology Roadmap*[2] cite numerous examples in aluminum refining of where thermochemical modeling could be applied to directly address key technology needs. The highest priorities are for: more durable refractories and coatings for the containment and transfer of molten metal and development of inert anode and wettable cathode materials. Both activities would benefit from an ability to predict stability of the base material, and especially grain boundary phases, providing guidance for new refractory design and behavior prediction. A third important problem that could be addressed by thermochemical modeling is the identification of additives for the suppression of molten metal/oxygen reactions to minimize dross and skim losses during melt/remelt operations.

Chemicals manufacturing: The chemical industry has significant needs in understanding behavior of materials of construction in extreme environments. This has been recognized through the establishment of the ASSET program, which involves a consortium of chemical companies, to establish and maintain a corrosion-behavior database linked with a thermochemical computational capability. An important element of this effort, the development of thermochemical data and relationships, has been recognized, but is yet to be addressed. Given high priority in the *Technology Roadmap for Materials of Construction in the Chemical Processing Industries*[3] are materials with high temperature/corrosion protection capabilities. Also indicated as important are high temperature refractory materials and prediction of material performance in complex systems. These all require capability for accurate thermochemical modeling, including reliable thermochemical data.

Glass manufacturing: The need for new refractories with improved performance is clearly highlighted in the *Glass Technology Roadmap Workshop Report* (1997)[4]. Both the Production Efficiency and Energy Efficiency working groups cite the "lack of cost-effective materials that perform adequately in glass furnace environments" as a key technology barrier and the need to better understand refractory decomposition, particularly "...in the oxy-fuel environment" as the most important materials research need. In addition to refractories, there is a need to develop new electrode materials for melters that are inert in the corrosive glass melt. Finally, the report cites the lack of fundamental knowledge concerning glassmaking and calls for improved models of glass melting, which includes accurate understanding of the thermal properties of the molten glass itself.

Glass coating: A need for fundamental data concerning glass-coating chemistries has been listed as a high-priority[5]. All four industry segments—flat, container, fiber, and specialty—agree on this point and cite the absence of such data as contributing to difficulties in process modeling and scale-up. The flat- and specialty-glass segments have particularly strong needs in this area, since the time required to develop and market new products must be reduced for them to remain competitive. Thermodynamic data are needed to predict chemical reaction rates, identify stable material phases, and ultimately, to model deposition processes and predict film thickness and uniformity. A desire for interactive databases containing information on deposition chemistries, which would include thermodynamic data, was indicated by all four segments.

Modeling of problems in materials corrosion, synthesis, and process modeling requires thermodynamic properties for many compounds. Data of high accuracy ($\pm$ 8-12 kJ mol^{-1}) are needed to perform useful simulations of reaction environments. The high temperatures at which corrosion and materials manufacturing occur, often in combustion environments, result in the production of a large number of very reactive gas-phase species. A wide range of construction materials are used, including refractories as well as metals. Multicomponent glasses are either the initial manufactured product or are produced by corrosion processes.

The three primary sources of thermochemical data cannot meet current IOF needs due to either lack of data for important species/compound classes or inaccurate information. The *JANAF Thermochemical Tables* are currently maintained by the National Institute of Standards and Technology (NIST). Although recently updated (1998), they still contain data based on experimental measurements published decades ago, while ignoring recent (and more accurate) theoretical and experimental investigations. For example, there are major errors in the heats of formation for silicon-containing species (which are very important for understanding refractory corrosion and glass making), and many important materials systems, particularly in the condensed phase, are not included. A Russian compilation known as *IVANTHERMO*, was published in 1989. This compilation corrects some of the errors in *JANAF*, but was never completed and is limited to main-group compounds. No data for transition-metal compounds are present and only simple condensed-phase oxides and halides are included. Finally, the SGTE database, a European compilation, is updated more regularly. SGTE has a strong emphasis on light metal alloys and molten salts; however, data for a number of important refractory corrosion problems are either not included or are incomplete. None of the databases contain information concerning liquid-phase products of refractory corrosion, which have been shown to be critical to the understanding of refractory corrosion in glass-melting furnaces (Allendorf and Spear, 2001)[6]. Data in all three compilations for reactive gas-phase intermediates are often highly inaccurate, as shown in Table I; errors > 40 kJ mol^{-1} exist in some cases.

Table 1. *Comparison of predicted heats of formation for some important high-temperature gas-phase intermediates with values in two commonly used databases (kJ mol^{-1}).*

Molecule	Predicted value[a]	JANAF	IVANTHERMO
$SiCl_3$	-318.1	-390.6	-336.6
SiF_3	-994.8	-1085.8	-996.7
SiF_2	-623.7	-588.1	-593.2
SiO	-111.8	-100.5	-76.6
SiO_2	-282.1	-305.6	-322.3
BCl_2	-38.1	-79.5	-61.1
$AlCl_2$	-224.8	---	-279.6
$InCl_2$	-126.4	---	-201

[a] Values obtained from high-level quantum chemistry calculations (BAC-MP4 calculation; see discussion below). All predicted heats of formation are in good agreement with recent experimental findings.

2.2 Project Objectives and Summary of Results

There were three tasks outlined in this project, each of which had its own set of objectives.

Task 1:Thermodynamic modeling of condensed-phase systems

The objective of this task was to expand the associate species model, which had already been proven to be an effective method of modeling high-temperature refractory systems, so that it could be used to generate thermodynamic properties for virtually all major ceramic-refractory chemistries used today. Most of these are oxide systems and as such they also include most of the components used in modern glass making. Thus, this task also provided data useful in modeling glass melts, as well as refractory synthesis and corrosion. The results are as follows:

- Highly accurate models for a base glass system of fundamental interest to glass and refractory manufacturers have been developed that include Na-Ca-Al-B-Si.
- A database has been developed contains Na-Ca-Al-Cr-B-Si-O, which will be of particular importance for alumina-chromia refractories typically used in gasifiers, combustors, and steel production.
- A database for the system Na-Al-Fe-B-Si-O has been developed that will allow calculations of interest in general refractory corrosion in the glass and aluminum industries.
- A high-accuracy model predicting phase equilibria in the Li_2O-Al_2O_3 system has been developed.
- A complete model for the Zr-Cr-Ca-Si-Al-Na-O-B is now available, with extensive new information regarding zirconia-containing systems.

Task 2: Prediction of high-temperature thermochemistry of gas-phase species

The objective of this task was to address the need for gas-phase thermochemical data for species, which are expected to play an important role in high-temperature refractory corrosion, material synthesis, and glass making. The previously-existing BAC methods, which we had shown to be sufficiently accurate for the purposes of database generation, were modified to permit their application to compounds containing elements relevant to refractories. The work in this task was conducted at SNL, with in-kind support from collaborators at SRI and LLNL. Briefly, the following key results were obtained during the project:

- An extensive body of new data relevant to the glass industry was determined, including data for compounds containing the elements indium, tin, and antimony, all of which are used extensively in the formation of low-emissivity coatings.
- Data relevant to the high-temperature corrosion of metals and alloys by halides was determined. In particular, chlorides and fluorides of chromium, manganese, and iron were obtained. These data are relevant to corrosion problems across a range of industries. New computational approaches to predicting transition-metal thermochemistry were developed as a result of this work.
- An extensive investigation of the high-temperature corrosion of chromium by oxygen and steam resulted in new thermodynamic data for species involved in this process that were previously unavailable. In addition, a combined theoretical and experimental study conducted in collaboration with investigators at NASA/Lewis Research Center resolved a controversy concerning the identity and thermochemistry of the most critical gas-phase species involved in these processes.[30]
- High-accuracy data for oxides and hydroxides of alkali metals (Li, Na, K) and Group II metals (Be, Mg, Ca) were determined, which are important for modeling corrosion processes in pulp and paper mills.
- Missing data for boron-containing oxides and hydroxides were determined.
- Data for a broad range of other volatile main-group compounds were provided from previous investigations, including hydrides, oxides, and halides of B, C, N, Al, Si, many with relevance to problems in the chemical, metals processing, and refining industries.

Task 3: Database development

The objective of this task was to make the data generated in Tasks 1 and 2 as accessible and useful as possible. The current trend in the scientific and engineering communities is to do this via the Internet. Task 3 was broken down into subtasks as follows:

- A website accessible to outside users was developed.
- Data for both gas-phase and condensed-phase species was presented in the form of polynomial fits that can be imported directly into commonly used modeling software, including CHEMKIN®[7] and FactSage™[8].
- The capability for visualizing the three-dimensional structure of molecules in the database was incorporated.
- Data from the existing BAC-MP4 database at SNL was imported to the website.
- Newly generated data for main-group and transition-metal compounds was also imported to the website.

- Data for a total of 1017 gas-phase species and 11 condensed-phase systems are available on the site.

3.0 COMPUTATIONAL METHODS USED TO GENERATE DATA

3.1 Bond-Additivity Correction

The thermodynamic and other molecular properties found in the gas-phase database are all obtained from Bond Additivity Correction (BAC) calculations, a class of quantum-chemistry based methods developed by C.F. Melius, in collaboration with P. Ho and M.D. Allendorf, and described in detail in various publications[9-12]. The BAC methods are based on the assumption that errors in electronic energies obtained from ab initio calculations are due to the finite size of the basis sets used and the application of limited electron correlation in the calculations. These errors are therefore systematic and can be corrected to achieve much greater accuracy for predicted heats of formation by applying a variety of empirical corrections related to the elements and bonds in the molecule.

The BAC suite of methods currently comprises several levels of theory. The most widely applied is the BAC-MP4 method, which was developed first. In this method, the molecular electronic energy is obtained from an ab initio electronic-structure calculation at the level of fourth-order Møller-Plesset perturbation theory. Methods using second-order Møller-Plesset perturbation theory (BAC-MP2), G2 theory (BAC-G2), and a hybrid method involving both density functional theory and MP2 have also been developed; these use a different approach for determining the empirical corrections to the ab initio electronic energy than the original BAC-MP4 method.

3.2 Coupled Cluster methods

The BAC method just described requires accurate heats of formation for at least one compound containing each of the bond types of interest. Unfortunately, accurate experimental data are often unavailable or conflicting, leading to very high uncertainties in the predictions of models developed to understand high-temperature processes such as corrosion. This is particularly true for transition-metal compounds that are important for understanding the high-temperature behavior of metals and alloys in corrosive environments. Computational approaches can help resolve inconsistencies among experimental data and fill gaps in the knowledge base. In this project we used coupled-cluster methods and large basis sets to determine thermochemical data for a number of halides, oxides, and hydroxides of tin, chromium, manganese, and iron. Agreement between the limited experimental data available and the predicted heats of formation is generally good, lending confidence to the overall theoretical approach.

Typically, molecular geometries were optimized and harmonic vibrational frequencies computed using B3LYP density functional theory with a triple-zeta basis set including diffuse and polarization functions. In some cases, optimizations were also carried out at the CCSD(T) level of coupled cluster theory using large basis sets to establish the shape of the ground state. Heats of

formation are computed by means of the CCSD(T) method in conjunction with high-quality basis sets, including corrections for core-valence correlation and scalar relativistic effects. Finally, we computed thermodynamic data over a range of temperatures using statistical mechanics. Details of these calculations can be found in these references[13-15].

3.3 Associate Species Model

A modified associate species approach is used to model the liquid phase in oxide systems. The relatively simple technique treats oxide liquids as solutions of end-member and associate species. The model was extended to representing glasses by treating them as under-cooled liquids. Equilibrium calculations using the model allow determination of species activities, phase separation, precipitation of crystalline phases, and volatilization. In support of nuclear waste glass development a model of the Na_2O-Al_2O_3-B_2O_3-SiO_2 system was developed which accurately reproduces its phase equilibria. The technique was applied to the CaO-SiO_2 system, which is used to demonstrate how two immisicible liquids can be treated.

4.0 WEBSITE DESCRIPTION

The website created during this project is http://www.ca.sandia.gov/HiTempThermo. The focus of this site is a database that provides thermochemistry for gas-phase and condensed-phase species relevant to a wide range of high-temperature processes, including chemical vapor deposition (CVD), chemical vapor infiltration (CVI), catalysis, combustion, materials corrosion, and aerosol processing.This database includes thermodynamic data (heats of formation, enthalpies, entropies, and heat capacities) for gas and condensed-phase species, thermodynamic models for specific condensed-phase material systems that account for non-ideal behavior in those systems, and a wide range of calculated molecular properties for gas-phase species.

4.1 Homepage

As with any website, the homepage is the first page the users see. It gives basic information about the project and has direct links to both the gas-phase and condensed-phase databases. It also links to explanations of the calculation methods used to create the data. The homepage includes sponsor information and contact information for the principal investigators.

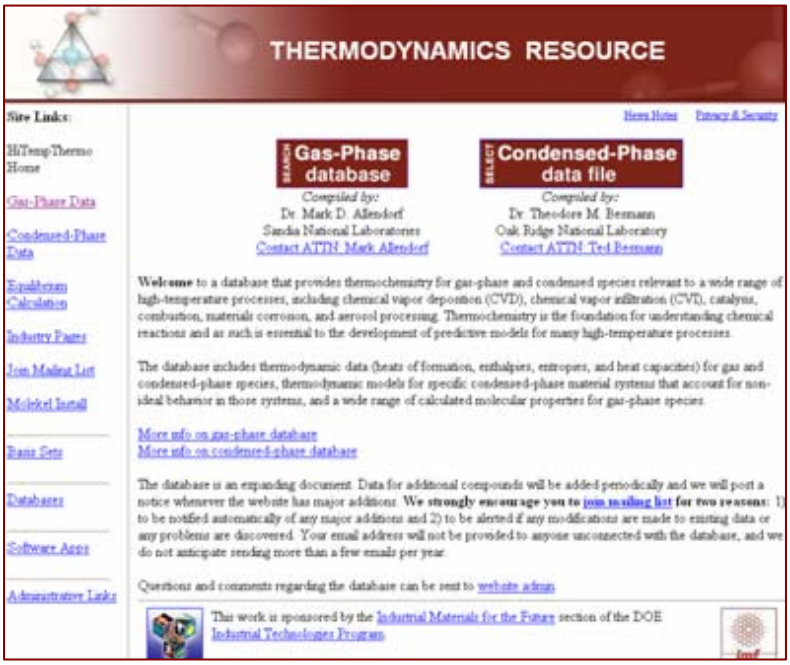

4.2 Gas-phase Data

The gas-phase database includes thermodynamic data and a wide range of calculated molecular properties. The data can be accessed either through a search for an individual molecule or groups of molecules or by selecting a molecule from an index. Once a molecule is selected, there are usually two pages of detailed thermodynamic information. Under the name of the molecule and the date that the data was put online is an option to view "previous uploads". This option is solely for reference purposes, as the data presented in the "previous uploads" is out of date. Another link allows the user to view the molecule with the Molekel software. The first data presented are the CHEMKIN® coefficients. These are formatted to be input directly into CHEMKIN®. An explanation of the format is available. More thermodynamic data follows: $\Delta H_f°(298)$, $S°(298)$, and $\Delta G°$ at six temperatures. After some notes on the molecule, including references and other information, a application is available to calculate [$H°(T) - H°(298)$], $S°$, and C_p at temperatures within the range (300 - 4000K). The calculation uses the polynomial fit given for this molecule. The second page of data lists the following information: moments of inertia, frequencies, hindered rotors (if applicable), atomic coordinates, symmetry, charge, multiplicity, and calculated electronic energies at various levels of theory. The final table is the thermodynamic data as a function of temperature and is a direct result of the BAC calculation and was used to fit the CHEMKIN® coefficients listed previously. This data may also be used to create fits according to the user's needs.

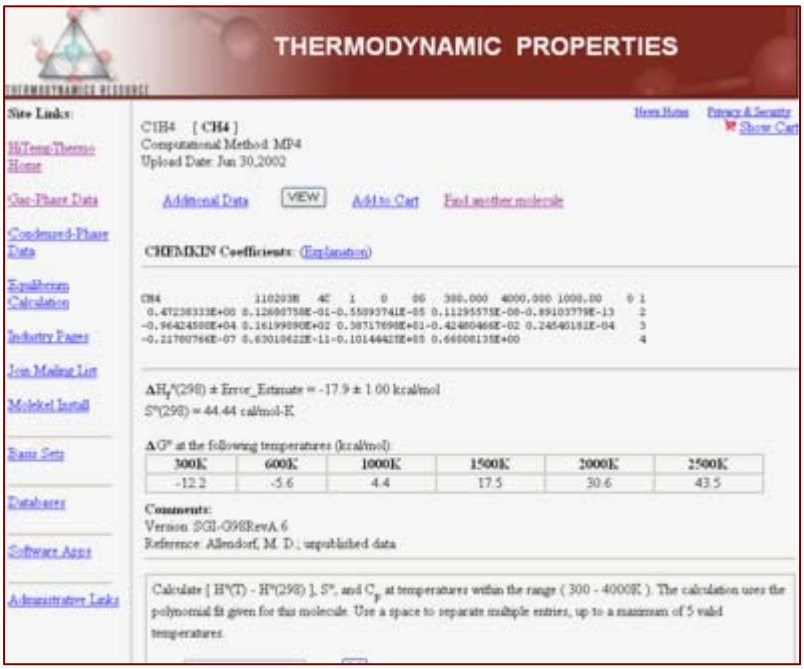

4.3 Condensed-phase Data

The data is accessed by selecting a system from a list and downloading the information. The condensed-phase data is presented in FactSage™ format so that it may be used as direct input into that software. There are several different systems available and an explanation of the format is listed on the condensed-phase data page. The information on each species includes the heat of formation, absolute entropy, heat capacity coefficients at different temperature ranges, and the heats of transition.

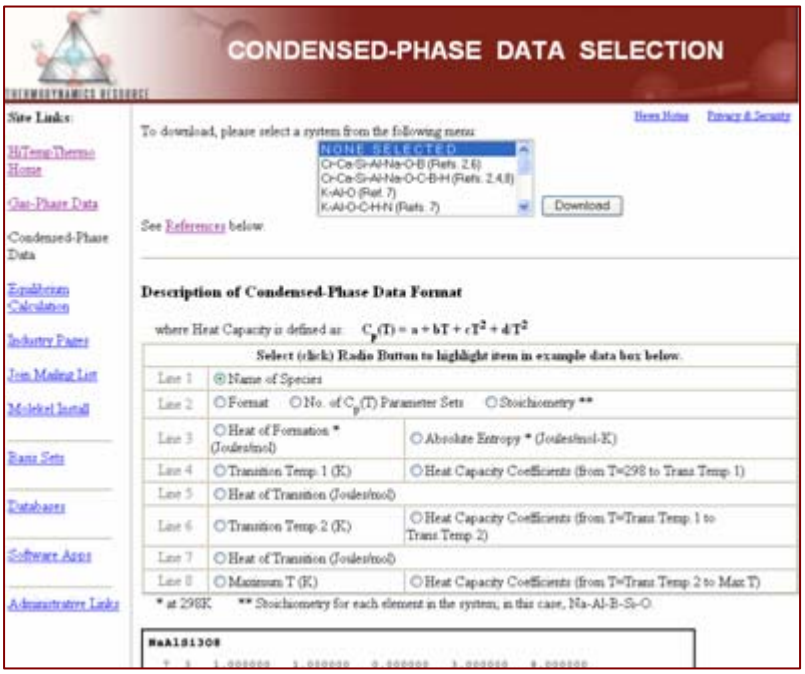

4.4 Equilibrium Calculators

The website includes relevant software to calculate equilibrium conditions with the data available on the site. CHEMKIN/EQUIL® is available to use with the gas-phase data. The purpose of this solver is to provide users of this web site with a tool for assessing the potential value of the data for understanding and modeling for their particular application. The solver also assists the user in becoming familiar with the use of thermodynamic data for solving high-temperature problems. A new equilibrium calculator based on the FactSage™ commercial software package was completed and is available on line for users. This calculator is designed to determine equilibria that includes condensed-phase systems, with both stoichiometric and solution-phase problems. All gas- and condensed-phase data available on our web site can be used in the calculations. This version of the FactSage™ Equil code is quite powerful, allowing users to perform a wide variety of equilibrium calculations, including fixed-activity, 2-phase immiscibility, and targeted calculations for liquidus and other phase formation.

4.5 Industry Pages

These pages contain data files tailored for specific industry problems: glass manufacturing, chemicals, petrochemical industry, and forest products. Their purpose is to collect from the large body of data in the data base only those species that are relevant to a particular problem and format the file so that it can be used as input to either the Factsage™ or CHEMKIN® programs. These files are in meant to be convenient, not comprehensive. Some species have been left out for the sake of compactness, particularly in cases where their equilibrium concentrations are

expected to be extremely small under typical processing conditions. Additional species can be added as needed by the user.

Glass Manufacturing: The soda-lime glass data file contains thermochemical information for the condensed phases and gaseous species in the Na-Ca-Si-O-C-H system. Four files are available for use in modeling the corrosion of various refractories used in glass melting furnaces. Eight files can be used to perform thermodynamic modeling of on-line deposition of tin oxide (SnO_2) using atmospheric pressure chemical vapor deposition (APCVD). One file is available to perform thermodynamic modeling of on-line deposition of titanium dioxide (TiO_2) using atmospheric pressure chemical vapor deposition (APCVD). Lastly, a data file provides thermochemistry for gas-phase species involved in the combustion of hydrocarbons under air- or oxygen-fired conditions.

Chemicals: There are four data files in this section. They relate to the following issues: hydrocarbon oxidation/pyrolysis, silane oxidation, silane pyrolysis, and diborane oxidation.

Petrochemical Industry: The GASIF data file for use with coal gasifiers problems contains the system Na-Ca-Al-Cr-Si-B-O-C-H. The chromia-alumina system is included so that refractory behavior can be considered. The global liquid phase is modeled using the modified associate species approach. End-member solid solutions were not modeled, and thus end-members are treated as stoichiometric compounds with no solubility for other components. There is a limited model for mullite restricted to Na_2O-AlO_2-SiO_2.

Forest Products: The development of black liquor gasification technology can substantially improve the energy efficiency of the pulp and paper industry. Gasification of black liquor with

combined-cycle cogeneration of steam and electricity requires improved materials, including the refractory liners of gasifier vessels. High alkali concentrations, high temperature (~950°C) and severe gas/liquid flow characteristics inside gasifiers combine for a challenging environment for refractory materials. Sodium reacts with the refractory causing expansion of the surface, spalling, and the development of other mechanical /structural refractory faults. The physical loss of as much as 40 percent of some refractory material has been observed. This degradation creates structural and safety problems, thermal efficiency losses, unacceptably high maintenance cost, and excessive downtime. To help understand and assess the issue, and to aid in the evaluation of alternative refractories, a relevant thermochemical datafile has been developed. It includes the magnesia-alumina spinel, which has been of interest as a more corrosion resistant material.

4.6 Additional Information

Mailing List: A voluntary mailing list exists for two reasons: 1) to notify users automatically of any major additions and 2) to alert users if any modifications are made to existing data or any problems are discovered.

3-D viewer – Molekel: This section includes instructions on how to install the free software, Molekel, so that the user may view the molecules on the site.

Other links: The website has links to other data available on the web, relevant software applications, and administrative information.

5.0 DESCRIPTION OF DATA

5.1 Gas-phase Data Systems

C-H-O[11]: The data in this system were calculated using the BAC-MP4 method.

B-N-Cl-H[16]: The data in this system were calculated using the BAC-MP4 method.

B-O-H: The data in this system were calculated using the BAC-MP4 method (unpublished).

B-Si-H[17]: The data in this system were calculated using the BAC-MP4 method. The reference compounds used in these calculations were silane, disilane, tetrachlorosilane, and BCl_3.

Si-C-H[18]: The data in this system were calculated using the BAC-MP4 method.

Si-C-Cl-H[10]: The data in this system were calculated using the BAC-MP4 method.

Si-N-F-H[10,19]: The data in this system were calculated using the BAC-MP4 method. The reference compounds used for these calculations were SiH_4, SiF_4, and Si_2H_6.

Si-O-H[20]: The data in this system were calculated using the BAC-MP4 method. The reference compounds used for these calculations were H_2O_2, O_2, and silane.

Al-H-C-O-F-Cl[21]: The data in this system were calculated using the BAC-G2 method. A correction to the aluminum reference state was made that affects the entropy and Gibbs free energy at temperatures < 933.45 K. The reference compounds for these calculations were AlH_3, AlF_3, $AlCl_3$, AlH, AlF, AlCl, and the constituent atoms.

Sn-H-O[13]: The data in this system were calculated using the BAC-MP4 method or the coupled clusters method.

Sn-H-C-Cl[22]: The data in this system were calculated using the BAC-MP4 method.

Cr-OH[15]: The data in this system were calculated using the coupled clusters method.

(Cr, Mn, Fe)-(F, Cl)[14]: The data in this system were calculated using the coupled clusters method.

In-C-H-O-Cl[23]: The data in this system were calculated using the BAC-MP4 method.

(Be, Ca, K, Li, Mg, Na)-O-H: The data in this system were calculated using the coupled clusters method.

Sb-H-C-O-Cl[24]: The data in this system were calculated using the BAC-MP4 method.

5.2 Condensed-phase Data Systems

The condensed-phase systems were calculated using the Associated Species Model. The references for these systems are listed below.

Cr-Ca-Si-Al-Na-O-B[25,26]

Cr-Ca-Si-Al-Na-O-C-B-H[25,27,28]

K-Al-O[29]

K-Al-O-C-H-N[29]

K-Si-O[6]

K-Si-O-C-H-N[6]

Na-Al-O[29]

Na-Al-O-C-H-N[29]

Na-Ca-Al-B-Si-O[25,27,28]

Na-Ca-Si-O-C-H-N[6,25]

Na-Si-O[6]

6.0 REFERENCES

(1) "Material Technologies for the Process Industries of the Future," available on line at www.nap.edu/catalog/10037.html#toc.

(2) "Aluminum Industry Technology Roadmap," http://www1.eere.energy.gov/industry/aluminum/pdfs/al_roadmap.pdf

(3) "Technology Roadmap for Materials of Construction in the Chemical Processing Industries", http://www.eere.energy.gov/industry/chemicals/pdfs/materials_tech_roadmap.pdf

(4) "Glass Technology Roadmap Workshop Report (1997)".

(5) Allendorf, M. D., "Research Needs for Coatings on Glass. Summary of the U.S. Department of Energy Roadmapping Workshop" *Thin Solid Films* **2001**, *392*, 155.

(6) Allendorf, M. D.; Spear, K. E., "Thermodynamic Analysis of Refractory Corrosion in Glass Melting Furnaces" *Journal of the Electrochemical Society* **2001**, *148*, B59.

(7) "Reaction Design", http://www.reactiondesign.com

(8) "FactSage", http://www.factsage.com

(9) Ho, P.; Coltrin, M. E.; Binkley, J. S.; Melius, C. F., *Journal of Physical Chemistry* **1985**, *89*, 4647.

(10) Ho, P.; Melius, C. F., *Journal of Physical Chemistry* **1990**, *94*, 5120.

(11) Melius, C. F. Thermochemistry of Hydrocarbon Intermediates in Combustion: Application of the BAC-MP4 Method. In *Chemistry and Physics of Energetic Materials*; Bulusu, S. N., Ed.; Kluwer Academic Publishers: Dorderecht, 1990; Vol. 309; pp 21.

(12) Melius, C. F.; Allendorf, M. D., *Journal of Physical Chemistry* **2000**, *104*, 2168.

(13) Nielsen, I. M. B.; Janssen, C. L.; Allendorf, M. D., "Ab initio predictions for thermochemical parameters for tin-oxygen compounds" *Journal of Physical Chemistry A* **2003**, *107*, 5122.

(14) Nielsen, I. M. B.; Allendorf, M. D., "High-level ab initio thermochemical data for halides of chromium, manganese, and iron" *Journal of Physical Chemistry A*, *109*, 928-933.

(15) Nielsen, I. M. B.; Allendorf, M. D., "Thermochemistry of the chromium hydroxides Cr(OH)n, n = 2-6, and the oxyhydroxide CrO(OH)4" *Journal of Physical Chemistry A* **2006**, *110*, 4093-4099.

(16) Allendorf, M. D.; Melius, C. F., *Journal of Physical Chemistry A* **1997**, *101*, 2670.

(17) Ho, P.; Colvin, M. E.; Melius, C. F., *Journal of Physical Chemistry A* **1997**, *101*, 9470.

(18) Allendorf, M. D.; Melius, C. F., *Journal of Physical Chemistry* **1992**, *96*, 428.

(19) Ho, P.; Melius, C. F., *Journal of Physical Chemistry* **1991**, *95*, 1410.

(20) Allendorf, M. D.; Melius, C. F.; Ho, P.; Zachariah, M. R., *Journal of Physical Chemistry* **1995**, 15285.

(21) Allendorf, M. D.; Melius, C. F.; Cosic, B.; Fontijn, A., *Journal of Physical Chemistry A* **2002**, *106*, 2629-2640.

(22) Allendorf, M. D.; Melius, C. F., "BAC-MP4 Predictions of Thermochemistry for Gas-Phase Tin Compounds in the Sn-H-C-Cl System" *Journal of Physical Chemistry A* **2005**, *109*, 4939.

(23) Skulan, A. J.; Nielsen, I. M. B.; Melius, C. F.; Allendorf, M. D., "BAC-MP4 Predictions of Thermochemistry for Gas-Phase Indium Compounds in the In-H-C-O-Cl System" *Journal of Physical Chemistry A* **2006**, *110*, 281.

(24) Skulan, A. J.; Nielsen, I. M. B.; Melius, C. F.; Allendorf, M. D., "BAC-MP4 Predictions of Thermochemistry for Gas-Phase Antimony Compounds in the Sb-H-C-O-Cl System" *Journal of Physical Chemistry A* **2006**, *110*, 5919.
(25) Besmann, T. M.; Kulkarni, N. S.; Spear, K. E. "Thermochemical And Phase Equilibria Property Prediction For Oxide Glass Systems Based On The Modified Associate Species Approach"; High Temperature Corrosion and Materials Technology IV, 2004, Pennington, NJ.
(26) Besmann, T. M.; Spear, K. E., "Thermochemical Modeling of Oxide Glasses" *Journal of the American Ceramic Society* **2002**, *85*, 2887.
(27) Besmann, T. M.; Kulkarni, N. S.; Spear, K. E., "Thermochemical Analysis and Modeling of the Al2O3-Cr2O3, Cr2O3-SiO2, and Al2O3-Cr2O3-SiO2 Systems Relevant to Refractories" *submitted to the Journal of the American Ceramic Society*.
(28) Spear, K. E.; Besmann, T. M.; Allendorf, M. D. "Modeling the Equilibrium Behavior of Chemically Complex Oxide Glass Solutions"; High Temperature Corrosion and Materials Chemistry V.
(29) Spear, K. E.; Allendorf, M. D., "Thermodynamic Analysis of Alumina Refractory Corrosion by sodium or potassium hydroxide in glass melting furnaces" *Journal of the Electrochemical Society* **2002**, *149*, B551-B559.
(30) E. J. Opila, D. L. Myers, N. S. Jacobson, I. M.B. Nielsen, D. F. Johnson, J. K. Olminsky and M. D. Allendorf "Theoretical and Experimental Investigation of the Thermochemistry of $CrO_2(OH)_2(g)$," *J. Phys. Chem. A,* **111** (2007), 1971.

7.0 APPENDIX A

7.1 Introduction to the BAC methods

The thermodynamic and other molecular properties found in this database are all obtained from Bond Additivity Correction (BAC) calculations, a class of quantum-chemistry based methods developed by C.F. Melius, in collaboration with P. Ho and M.D. Allendorf, and described in detail in various publications.[1-4] The BAC methods are based on the assumption that errors in electronic energies obtained from *ab initio* calculations are due to the finite size of the basis sets used and the application of limited electron correlation in the calculations. These errors are therefore systematic and can be corrected to achieve much greater accuracy for predicted heats of formation by applying a variety of empirical corrections related to the elements and bonds in the molecule.

The BAC suite of methods currently comprises several levels of theory. The most widely applied is the BAC-MP4 method, which was developed first. In this method, the molecular electronic energy is obtained from an *ab initio* electronic-structure calculation at the level of fourth-order Møller-Plesset perturbation theory. Methods using second-order Møller-Plesset perturbation theory (BAC-MP2), G2 theory (BAC-G2), and a hybrid method involving both density functional theory and MP2 have also been developed; these use a different approach for determining the empirical corrections to the *ab initio* electronic energy than the original BAC-MP4 method.

7.2 The BAC-MP4 method

The BAC-MP4 method is shown schematically in Figure 1; the individual calculations are described below. All calculations were performed using the Gaussian suite of quantum-chemistry codes;[5] the precise version of the code used for a particular MP4 calculation is given in the database in most cases.

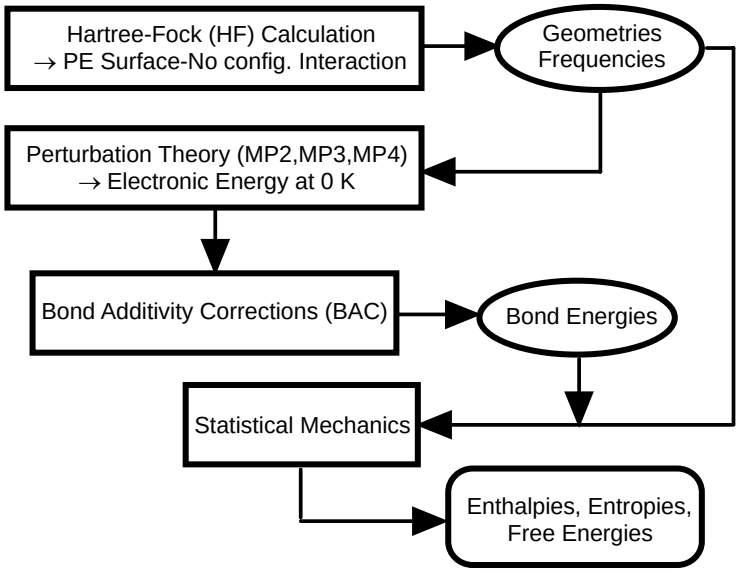

Figure 1. Schematic of the BAC Method

Molecular geometries, vibrational frequencies, and moments of inertia. The molecular equilibrium geometry is required input for the MP4 calculation used in the BAC-MP4 method. This geometry and the frequencies and moments of inertia derived from it are also used in post-*ab initio* calculations to obtain thermodynamic data at temperatures above 0 K.

In the BAC-MP4 method, equilibrium geometries and harmonic vibrational frequencies are obtained from Hartree-Fock (self-consistent field) theory (an introduction to these and other quantum-chemistry methods can be found in Ref. 6). Restricted Hartree-Fock theory (RHF) is used for closed shell molecules and unrestricted Hartree-Fock theory (UHF) is used for open-shell molecules, using the 6-31G(d) basis set. Vibrational frequencies calculated at this level of theory are known to be systematically larger than experimental values; thus, each calculated frequency is scaled by dividing it by 1.12.[7]

Electronic energies. To determine atomization enthalpies and thus heats of formation, the effects of electron correlation are included by performing single-point calculations, using Møller-Plesset perturbation theory (MP4 using the 6-31G(d,p) basis set with single, double, triple and quadruple substitutions) and the HF/6-31G(d) geometries.

Bond additivity corrections and corrected heats of formation. The form of the BAC parameters α_{ij}, A_{ij}, and B_k used to calculate the corrections for individual molecules is given in Equations 1-4, using the example of a bond between atoms X_i and X_j in a molecule of the form X_k-X_i-X_j :

$$E_{BAC}(X_i\text{-}X_j) = f_{ij}g_{kij} \quad (1)$$

where

$$f_{ij} = A_{ij}\exp(-\alpha_{ij}R_{ij}) \quad (2)$$

$$g_{kij} = (1. - h_{ik}h_{ij}) \quad (3)$$

$$h_{ik} = B_k\exp\{-\alpha_{ik}(R_{ik} - 1.4\ \text{Å})\} \quad (4)$$

A_{ij} and α_{ij} are empirically derived parameters that depend on the X_i-X_j bond type and R_{ij} is the bond distance (Ångstroms). The factor B_k in Equation 4 is used to derive a correction for the effects of neighboring atoms on the X_i-X_j bond (Equation 3) and depends on the identity of atom k.

A correction is also made in the case of open-shell molecules for spin contamination of the ground state by excited electronic states. The error in the electronic energy caused by this effect was estimated using the approach of Schlegel[8] and is given by

$$E_{BAC}(\text{spin } S^2) = E(\text{UMP3}) - E(\text{PUMP3}) \quad (5)$$

where E(UMP3) is the third-order MP energy using the UHF wavefunction and E(PUMP3) is the projected UMP3 energy. This correction is generally small (~ 0.5 kcal mol^{-1}) but may become large for molecules containing a high degree of unsaturation or low-lying electronic excited

states. Closed-shell molecules that are UHF-unstable, such as SiH_2, also require an additional correction. The form of the correction is:

$$E_{\mathrm{BAC}}(\mathrm{spin}_{\mathrm{UHF\text{-}unstable}}) = K_{\mathrm{UHF\text{-}I}} S(S+1) \qquad (6)$$

where $K_{\mathrm{UHF\text{-}I}}$ is 10.0 kcal mol^{-1} (based on the heat of formation of O_3) and S is the spin obtained from the UHF/6-31G(d,p) calculation. Application of this correction yields reasonable heats of formation for singlet SiH_2 and CH_2.

Table A-1 (following page) lists the parameters A_{ij}, α_{ij} and B_k used in this work for each bond type, all of which were determined previously. References are also given where detailed information can be found concerning the basis used for establishing these values.

Table A-1. *BAC Parameters for the BAC-MP4 (SDTQ) Level of Theory.*

Bond	A_{ij} (MP4)[a]	α_{ij}(MP4)[b]	Reference
H-H	18.98	2.000	3
B-H	31.12	2.000	9
B-B	969.88	3.800	10
B-N	370.10	2.840	9
B-F	206.89	2.650	11
B-Si	45.77	1.000	10
B-Cl	172.49	2.000	9
C-H	38.61	2.000	11
C-C	1444.09	3.800	11
C-N	462.33	2.800	11
C-O	175.62	2.141	11
C-F	143.29	2.100	11
C-Cl	304.26	2.000	11
N-H	70.08	2.000	11
N-N	472.62	2.600	11
N-O	226.04	2.100	11
O-H	72.45	2.000	11
O-O	169.78	2.000	11
Si-H	92.79	2.000	1,12
F-H	84.21	2.000	11
F-N	170.05	2.000	11
F-O	189.70	2.000	11
F-F	129.17	2.000	11
Si-C	893.71	2.500	13
Si-N	847.99	2.500	14
Si-O	7038.50	3.978	15
Si-F	260.65	2.000	2
Si-Si	3330.21	2.700	12
Si-Cl	721.93	2.000	1
Cl-H	116.40	2.000	11
Cl-O	355.14	2.000	11
Cl-Cl	980.18	2.000	11
In-H	164.1	2.000	16
In-C	528.1	2.000	16
In-O	319.1	2.000	16
In-Cl	924.0	2.000	16
Sn-H	147.39	2.000	17
Sn-C	472.71	2.000	17
Sn-O	622.53	2.000	11
Sn-Cl	951.85	2.000	17
Sb-H	244.1	2.000	18
Sb-C	649.4	2.000	18
Sb-O	639.5	2.000	18
Sb-Cl	1718.7	2.000	18

[a] In kcal mol^{-1}

[b] In $Å^{-1}$

Table A-1 *(cont'd)*

Atom	B_k(MP4)	Atom	B_k(MP4)
H	0.0	In	0.30
B	0.200	Sn	0.30
C	0.310	Sb	0.30
N	0.200		
O	0.225		
F	0.330		
Si	0.2		
Cl	0.42		

Table A-2. *Atomic heats of formation (0 K), kcal mol^{-1}, used to calculate heats of formation.*

Atom	ΔH_{f0}^{o}	Reference
H	51.63	19
B	133.8	20
C	169.98	19
O	58.99	19
N	112.53	19
F	18.48	19
Si	106.66	19
Cl	28.59	19
In	57.63	20
Sn	72.014	20
Sb	62.63	21

Atomization energies and heats of formation at 0 K. The sum of the BACs is combined with the MP4(SDTQ) electronic energy and the unscaled zero-point energy to obtain the heats of atomization and formation at 0 K (ΣD_O and $\Delta H°_f$(0 K), respectively). Values of the atomic heats of formation used in this calculation are given in Table A-2.

The corrected $\Delta H°_f$(0 K) is obtained as follows. First, the calculated molecular electronic energy is added to the zero-point energy (calculated from the unscaled vibrational frequencies). Next, the resulting energy is subtracted from the calculated electronic energies of the atoms to give an electronic heat of atomization:

$$E_{\text{atomization}} = \sum_{i}^{n} E_i(\text{atoms}) - (E_{\text{ab initio}}(\text{molecule}) + E_{\text{ZPE}}) \qquad (7)$$

Referencing this energy against the experimental $\Delta H°_f$ (0 K) of the atoms in the gas phase (Table A-2) yields the uncorrected molecular $\Delta H°_f$ (0 K):

$$\Delta H^\circ_{f0,\ \text{uncorrected}} = \sum_{\text{atoms}} \Delta H^\circ_{f0,\ \text{atoms}} - E_{\text{atomization}} \qquad (8)$$

Subtracting the BAC corrections from this energy finally yields the corrected (BAC-MP4) $\Delta H°_f$ (0 K):

$$\Delta H^\circ_{f0,\text{BAC}} = \Delta H^\circ_{f0,\text{uncorrected}} - E_{\text{BAC-Correction}} \qquad (9)$$

Thermodynamic data as a function of temperature. Entropies, heat capacities, enthalpies, and free energies as a function of temperature are calculated using the heats of formation at 0 K, moments of inertia, and vibrational frequencies. Equations derived from statistical-mechanics, an extension of the subroutines in the Gaussian codes, are employed.[5] These subroutines use standard expressions for an ideal gas in the canonical ensemble to compute the heat capacity, enthalpy, and entropy. For consistency with previous work, unscaled frequencies are used to determine ΔH°_f (0 K), while the scaled frequencies are used to calculate thermochemistry at higher temperatures. Minor differences that would result from using the scaled frequencies to calculate ΔH°_f (0 K) are incorporated into the BACs. Vibrations are assumed to be harmonic at all temperatures.

To calculate the heat of formation, Gibbs free energy of formation, and equilibrium constant as a function of temperature, the temperature-dependent enthalpy and entropy of the elements in their standard state is required. For diatomic gas-phase molecules, we calculate these quantities using analytical expressions derived from statistical mechanics and the scaled vibrational frequency predicted at the HF/6-31G(d) level. This introduces some error in the data at very high temperatures (> 1500 K; see Error Estimates below). Reference-state data for nongaseous elements were obtained by fitting thermodynamic functions published in either the *JANAF Thermochemical Tables*[19] or in *Thermodynamic Properties of Individual Substances* [20] (data for In, Sn, and Sb only).

Treatment of Hindered Rotors. Contributions to the heat capacity and entropy from rotating groups are accounted for by substituting a hindered rotor for the corresponding vibrational frequency determined by the HF calculation. Approximate analytical functions have been developed to estimate the hindered rotor energy E_{hr}, heat capacity C_{hr}, and entropy change ΔS_{hr}.[22] The expressions are

$$E_{hr} = RT\ (\ 1/2 + Y - g(Y)\ )\ (\ x / (e^x - 1) \qquad (10)$$

$$C_{hr} = R\ (\ 1/2 + Y^2 - g(Y)\ - g(Y)^2\ )\ (\ x^2 / (e^x - 1)^2\ ) \qquad (11)$$

$$\Delta S_{hr} = R\ (\ \ln(SI_0) + Y - g(Y)\ )\ (\ z^2\ e^z / (e^z - 1)^2\ ) \qquad (12)$$

where

$$g(Y) = Y (SI_1 / SI_0) \quad (13)$$

$$Y = V / 2RT \quad (14)$$

$$x = (1.67 / I_r) \text{ sqrt } (V / RT) \quad (15)$$

and

$$z = 3.8 / I_r \quad (16)$$

where $SI_m(Y)$ is the scaled modified Bessel function of order m. The expressions in eqns. 10 - 12 are exact for $I_r \rightarrow \infty$, as derived by Pitzer and Gwinn.[22] Eqns. 10 - 12 do an excellent job of fitting the tabulated values of ref. 18 for I_r's of chemical interest. The largest error is in determining the barrier height V and the rotational "degeneracy" for non-symmetrical functional groups.

Error estimates. There are two major sources of uncertainty in the calculated heats of formation: 1) uncertainties resulting from the applicability of the theoretical methods to a given molecule and 2) systematic uncertainties resulting from lack of good reference compounds for the BACs. The magnitude of the first is estimated using an *ad hoc* method developed previously that uses the results from lower-level calculations[2] and is provided on the web site for each molecule in the data base:

$$Error(\text{BAC-MP4}) = \{1.0 \text{ kcal mol}^{-1} + (\Delta H_{\text{BAC-MP4}} - \Delta H_{\text{BAC-MP3}})^2 + (\Delta H_{\text{BAC-MP4}} - \Delta H_{\text{BAC-MP4SDQ}})^2 + 0.25(E_{\text{BAC}}(\text{spin}_S{}^2) \text{ or } E_{\text{BAC}}(\text{spin}_{\text{UHF-I}}))^2\}^{1/2} \quad (17)$$

The second source of uncertainty can add a few kcal mol^{-1} to the uncertainty estimates and will scale with the number of bonds in the molecule. The use of different reference values would shift our calculated heats of formation as a group, with the consequence that calculated bond dissociation enthalpies and reaction enthalpies are affected less than the heats of formation.

Two other sources of error to be aware of are 1) the use of an analytical expression to calculate temperature-dependent thermodynamic data for the reference state of diatomic elements and 2) the assumption that elemental masses correspond to the mass of the most abundant isotope. The first results in errors that increase with temperature. For at temperatures ≤ 2000 K, errors of 0.16 cal mol^{-1} K^{-1}, 0.18 kcal mol^{-1}, and 0.26 cal mol^{-1} K^{-1} or less per atom exist in the Cp, H(T) – H(298 K), and S° relative to data for the elements H_2, N_2, O_2, Cl_2, and F_2 published in the *JANAF Tables*.[19] At 1000 K, the errors are only 0.10 cal mol^{-1} K^{-1}, 0.06 kcal mol^{-1}, and 0.18 cal mol^{-1} K^{-1}, respectively. The second source introduces only a very slight error. The effect is

largest for molecules containing chlorine and amounts to less than 0.1 kcal mol^{-1} in a molecule with four chlorine atoms.

Overall, we believe that the uncertainties in the BAC-MP4 heats of formation lie in the ± 2-5 kcal mol^{-1} range.

7.3 The BAC-G2 Method

Overview of the BAC-G2 method.

The BAC-G2 method[4] applies the BAC corrections to the standard G2 method,[23] using the Gaussian quantum-chemistry codes. The electronic-structure calculations to determine the geometry, vibrational frequencies, and electronic energies are the same as those in the G2 method. Specifically, the geometry and vibrational frequencies in the BAC-G2 method are obtained from a Hartree-Fock (HF) calculation (restricted Hartree-Fock, RHF, for closed shell molecules and unrestricted Hartree-Fock, UHF, for open shell molecules) using the 6-31G(d) split-valence basis set with polarization functions on the heavy (non-hydrogen) atoms. At this level of theory, vibrational frequencies are systematically too large compared to experimental values. We therefore scale the HF harmonic frequencies downward by 12 percent. The electronic energies at the QCI, MP4, and MP2 levels of theory, as well as the collective G1, G2MP2, and G2 electronic energies, are taken directly from the output of the G2 method. The basis sets are the same as those defined in the standard G2 method. The geometry used in the single-point calculations is obtained by reoptimizing the HF geometry at the MP2 level, again as defined in the G2 method.

BAC corrections. The BAC corrections for the BAC-G2 method are those defined previously.[4] Briefly, three types of corrections (E_{BAC-}; units of energy) are used: atomic, molecular, and bondwise, indicated in Equations (18)—(21) below. The atomic correction depends on the atom type:

$$E_{BAC\text{-}atom} = \sum_k E_{BAC\text{-}atom}(A_k) \tag{18}$$

where the sum runs over all the atoms in the molecule. The value of $E_{BAC\text{-}atom}$ (A_k) depends on the atom type and A_k is an adjustable parameter.

The molecular BAC correction arises from errors in the overall electronic structure of the molecule. The BAC correction for this term is given by

$$E_{BAC\text{-}molecule} = E_{BAC\text{-}elec\ pair} \tag{19}$$

where $E_{BAC\text{-}elec\ pair}$ depends on the difference between the spin of the molecule and the sum of the spins of the constituent atoms:

$$E_{BAC\text{-}elec\ pair} = K_{elec\ pair}(Spin_{molecule} - \sum_{atom} Spin_{atom}) \quad (20)$$

where $K_{Elec\ pair}$ is an empirically adjusted parameter for a given BAC method and "Spin" refers to the S quantum number.

The third type of BAC correction depends on the formation of chemical bonds. In this instance, we distinguish between bonds and pair-wise interactions. A bond is taken to mean the formation of an electron pair between the atoms. This correction addresses systematic errors arising from electron-pairing not covered by Eqn. 20. The correction for each bond A-B in the molecule having neighbors C and D (e.g., C-A-B-D) is given by

$$E_{BAC\text{-}bond}(AB) = A_{AB} e^{-\alpha R_{AB}} + \sum_{C} B_{CA} + \sum_{D} B_{DB}, \quad (21)$$

where the first term is the correction for the bond alone, while the corrections for its nearest neighbors are treated as a sum of corrections for each neighbor of the form

$$B_{CA} = B_C + B_A. \quad (22)$$

The B_A's are constants that depend only on the type of atom. The bond-distance dependence in Eqn. 21 exists only in the first term for the bond itself. Furthermore, α no longer depends on the type of bond, as it did in the original BAC method.[3] Note that the bond-wise corrections do not go to zero at infinity, due to the terms $\Sigma B_{CA} + \Sigma B_{DB}$ defined by Eqn. 22.

The parameters for each of the corrections are given in Table A-3; values of all parameters with the exception of those for aluminum (see below) were determined previously.[4] The atomic corrections (Eqn. 18) are straightforward. For the bond-wise corrections (Eqn. 21), the α exponent is taken to be 3.0 $Å^{-1}$, while the pre-exponential coefficient A_{AB} is taken to be the geometric mean of the individual atom types, i.e.,

$$A_{AB} = -(A_{AA} A_{BB})^{1/2} \quad (23)$$

Equation 21 also includes contributions from the nearest-neighbor B_{ij} terms (defined by Equation 22). The accuracy of the parameters comprising these terms (see Table A-3) is difficult to assess because of their small size. This is due to the fact that to date we have only applied the BAC-G2 method to relatively small molecules (less than seven heavy, i.e., non-hydrogen, atoms), for which accurate experimental thermodynamic data exist. However, these terms become quite significant for larger molecules and for halides (see below). Unfortunately, given the limited

accuracy of experimental data for larger non-hydrocarbon, unsaturated gas-phase species it will remain difficult to establish the accuracy of the B_{atom} terms.

Table A-3. *BAC-G2 Parameters (Energies in kcal-mol^{-1}) and atomic heats of formation used in the calculations of heats of formation.*

$K_{Elec\ pair} = 0.860$				ΔH_{f0}^{o} [a]
Atom	A_{Atom}	B_{Atom}	A_{ii}	
H	0.485	-0.146	1.462	51.15
C	1.081	0.051	0.0	168.90
N	1.498	-0.010	2.281	111.03
O	-0.501	-0.010	114.3	59.49
F	-1.942	0.215	373.1	20.41
Al	-1.500	0.000	300.0	79.73
Si	0.097	0.008	297.4	106.56
Cl	-0.776	0.087	1433.7	29.37

[a] Atomic heat of formation at 0 K, kcal mol^{-1}, obtained from the BAC-G2 method.

Heats of formation. The corrected heat of formation at 0 K (ΔH_{f0}^{o}) can now be obtained from the calculated electronic energy. First, the electronic energy is added to the zero-point energy (which is automatically included in the G2(0 K) output of the Gaussian-94 and Gaussian 98 codes). Next, the resulting energy is subtracted from the electronic energies of the atoms to give an electronic heat of atomization:

$$E_{\text{atomization}} = \sum_{i}^{n} E_i\,(\text{atoms}) - (E_{\text{ab initio}}\,(\text{molecule}) + E_{\text{ZPE}}) \tag{24}$$

Referencing this energy against the BAC-G2 ΔH_{f0}^{o} at 0 K of the atoms (given in Table A-3) in the gas phase yields the uncorrected ΔH_{f0}^{o}:

$$\Delta H^{\circ}_{\text{f0, uncorrected}} = \sum_{\text{atoms}} \Delta H^{\circ}_{\text{f0, atoms}} - E_{\text{atomization}} \tag{25}$$

Subtracting the BAC corrections from this energy finally yields ΔH_{f0}^{o} at 0 K:

$$\Delta H^{\circ}_{\text{f0, BAC}} = \Delta H^{\circ}_{\text{f0, uncorrected}} - E_{\text{BAC-Correction}} \tag{26}$$

Thermodynamic data as a function of temperature. Heats of formation, entropies, and free energies at various temperatures are then obtained using equations derived from statistical mechanics (the same procedure as in the original BAC-MP4 method, which includes corrections for hindered rotors, such as CH_3 groups; see discussion above). Thus, for finite temperatures, the raw G2 energies (without BAC corrections) obtained from the BAC-G2 method do not correspond to those from the output of a Gaussian G2 calculation, since hindered rotors are included in the BAC procedure.

Error estimates. Using an *ad hoc* expression similar to that formulated for the earlier BAC-MP4 method[2] we obtain an estimate of the error (or confidence level) in the BAC-G2 method. In this case, we use the similarities between the G1 and G2-MP2 methods and the G2 method itself as an indication of the error:

$$\text{Error (BAC-G2)} = \text{Sqrt } \{ 1.0 \text{ kcal-mol}^{-1} + (\Delta H_{\text{BAC-G2}} - \Delta H_{\text{BAC-G2MP2}})^2 + (\Delta H_{\text{BAC-G2}} - \Delta H_{\text{BAC-G1}})^2 \}. \quad (27)$$

7.4 REFERENCES

(1) Ho, P.; Coltrin, M. E.; Binkley, J. S.; Melius, C. F. J. Phys. Chem. 1985, 89, 4647.
(2) Ho, P.; Melius, C. F. J. Phys. Chem. 1990, 94, 5120.
(3) Melius, C. F. Thermochemistry of Hydrocarbon Intermediates in Combustion: Application of the BAC-MP4 Method. in Chemistry and Physics of Energetic Materials; Bulusu, S. N., Ed.; Kluwer Academic Publishers: Dorderecht, 1990; Vol. 309; pp 21.
(4) Melius, C. F.; Allendorf, M. D. J. Phys. Chem. 2000, 104, 2168.
(5) Frisch, M. J.; Trucks, G. W.; Schlegel, H. B.; Scuseria, G. E.; Robb, M. A.; Cheeseman, J. R.; Zakrzewski, V. G.; Montgomery, J., J. A.; Stratmann, R. E.; Burant, J. C.; Dapprich, S.; J. M. Millam; Daniels, A. D.; Kudin, K. N.; Strain, M. C.; Farkas, O.; Tomasi, J.; Barone, V.; Cossi, M.; Cammi, R.; Mennucci, B.; Pomelli, C.; Adamo, C.; Clifford, S.; Ochterski, J.; Petersson, G. A.; Ayala, P. Y.; Cui, Q.; Morokuma, K.; Malick, D. K.; Rabuck, A. D.; Raghavachari, K.; Foresman, J. B.; Cioslowski, J.; Ortiz, J. V.; Stefanov, B. B.; Liu, G.; Liashenko, A.; Piskorz, P.; Komaromi, I.; Gomperts, R.; Martin, R. L.; Fox, D. J.; Keith, T.; Al-Laham, M. A.; Peng, C. Y.; Nanayakkara, A.; Gonzalez, C.; Challacombe, M.; Gill, P. M. W.; Johnson, B.; Chen, W.; Wong, M. W.; Andres, J. L.; Gonzalez, C.; Head-Gordon, M.; Replogle, E. S.; Pople, J. A. Gaussian 98, Revision A.6; Gaussian, Inc.: Pittsburgh, 1998.
(6) Hehre, W. J.; Radom, L.; Schleyer, P. v. R.; Pople, J. A. Ab Initio Molecular Orbital Theory; Wiley: New York, 1986.
(7) Hariharan, P. C.; Pople, J. A. Theor. Chim. Acta 1973, 28, 213.
(8) Schlegel, H. B. J. Chem. Phys. 1986, 84, 4530.
(9) Allendorf, M. D.; Melius, C. F. J. Phys. Chem. A 1997, 101, 2670.
(10) Ho, P.; Melius, C. F. J. Phys. Chem. A 1997, 101, 9470.
(11) Allendorf, M. D.; Melius, C. F., unpublished data.
(12) Ho, P.; Coltrin, M. E.; Binkley, J. S.; Melius, C. F. J. Phys. Chem. 1986, 90, 3399.
(13) Allendorf, M. D.; Melius, C. F. J. Phys. Chem. 1992, 96, 428.
(14) Melius, C. F.; Ho, P. J. Phys. Chem. 1991, 95, 1410.
(15) Allendorf, M. D.; Melius, C. F.; Ho, P.; Zachariah, M. R. J. Phys. Chem. 1995, 99, 15285.
(16) Skulan, A. J.; Nielsen, I. M. B.; Melius, C. F.; Allendorf, M. D. J. Phys. Chem. A 2005, in press.
(17) Allendorf, M. D.; Melius, C. F. J. Phys. Chem. A 2005, 109, 4939.
(18) Skulan, A. J.; Nielsen, I. M. B.; Melius, C. F.; Allendorf, M. D. J. Phys. Chem. A 2005, submitted.
(19) Chase, M. W.; Davies, C. A.; Downey, J. R.; Frurip, D. J.; McDonald, R. A.; Szverud, A. N. J. Phys. Chem. Ref. Data 1985, 14.
(20) Gurvich, L. V.; Veyts, I. V.; Alcock, C. B. Thermodynamic Properties of Individual Substances; CRC Press: Boca Raton, 1994; Vol. 3.
(21) Wagman, D. D.; Evans, W. H.; Parker, V. B.; Schumm, R. H.; Halow, I.; Bailey, S. M.; Churney, K. L.; Nuttall, R. L. J. Phys. Chem. Ref. Data 1982, 11, Suppl. 2.
(22) Pitzer, K. S.; Gwinn, W. D. J. Chem. Phys. 1942, 10, 428.
(23) Curtiss, L. A.; Raghavachari, K.; Trucks, G. W.; Pople, J. A. J. Chem. Phys. 1991, 94, 7221.

8.0 APPENDIX B

8.1 Introduction to the Associate Species Model

Oxide glass materials have been in use for millennia, yet glass remains a highly enigmatic material. For example, the chemical thermodynamics of oxide melts, slags, and glasses have been difficult to model because of strong interactions between constituents, particularly with silica. Thus, unlike many metal alloys, simple solution models do not accurately reproduce the thermodynamic and phase relations in most oxide liquid systems. While lacking long-range order, oxide glass materials have very specific short-range/cluster periodicity that is a function of composition. Even oxide liquids exhibit short-range order and specific coordinations have been observed experimentally and computed using molecular dynamics. [1]

An approach has been developed that is a fairly simple method for modeling these amorphous systems, and it has been termed the modified associate species model. The associate species approach is attractive because it (a) accurately represents the thermodynamic behavior of very complex chemical systems over wide temperature and composition ranges, (b) accurately predicts the activities of components in metastable equilibrium glass phases, (c) allows logical estimation of unknown thermodynamic values with an accuracy much greater than that required for predicting useful engineering limits on thermodynamic activities in solutions, and (d) is relatively easy for non-specialists in thermochemistry to understand and use. Ideally mixing associate species accurately represent the solution energies in which end member components exhibit attractive forces. The modification to the associate species model, hence the term "modified" associate species model, is the incorporation of positive solution model constants to represent any positive interaction energies in a solution. With these it is possible to accurately represent reported immiscibility in solution phases (e.g., liquid-liquid immiscibility common in many silica containing systems). The result is simple, well-behaved equations for free energies that can be confidently extrapolated and interpolated into unstudied temperature and composition ranges.

8.2 Modified Associate Species Model

The associate species solution model uses intermediate "chemical species" with their corresponding thermodynamic data to represent the negative non-ideal mixing of the end-member components in a system. For example, liquid $NaAlO_{2(l)}$ and $Na_2Al_4O_{7(l)}$ species ideally mix with end-member $Na_2O_{(l)}$ and $Al_2O_{3(l)}$ to represent the liquid phase in the Na_2O-Al_2O_3 binary system. While $NaAlO_{2(l)}$ and $Na_2Al_4O_{7(l)}$ may not exist as chemical entities that can be isolated and characterized, these species in the model can accurately represent the negative interaction energies, that occur between soda and alumina in an oxide liquid solution.

All liquid associate species are written with formulae containing two non-oxygen atoms per mole, which equally weights each species with regard to its ideal mixing contribution. Thus, the

$Na_2Al_4O_7$(l) species noted above is actually $Na_{2/3}Al_{4/3}O_{7/3}$(l) or $Na_2Al_4O_7$:1/3(l) in the terminology used in the current work. This procedure was adopted during the optimization process when phase diagram information was being mathematically compared with thermodynamic data to obtain internally consistent sets of data for a given chemical system. It was determined that for all systems (aluminates, borates, silicates, aluminosilicates, etc.), the thermochemical data could more easily be optimized when liquid associate species contained two non-oxygen atoms per species rather than one. This procedure influences the ideal mixing energy of the solution phase, but the implications of its use are not yet fully understood. However, for very stable liquid associate species, no ideal mixing energy (ideal mixing entropy) exists at the composition of that associate since one single associate species makes up the entire liquid solution at that composition.

Complex, multi-component system models are built up from the constituent binary and ternary systems. Binary and ternary constituent systems are modeled so that they accurately represent the experimentally determined phase equilibria. The various associates of these binaries and ternaries can then be included in a single ideal solution for a large number of constituent oxides, allowing equilibria to be easily computed and chemical activities derived. Where liquid immiscibilities exist in the binary and ternary systems such that some interaction terms are necessary to accommodate repulsive energetic relationships, these too can be used in fairly straightforward data-files. Unlike the modified quasi-chemical model, these interaction terms rarely require more than one or two terms, which include temperature dependencies. Fitting the phase diagram can be accomplished by manually, obviating the need for sophisticated optimization routines.

8.3 Na_2O-Al_2O_3 System

A fundamental oxide system that is useful for illustrating the associate species approach is Na_2O-Al_2O_3. In using the associate species model to represent the thermodynamic properties of the liquid phase in the Na_2O-Al_2O_3 binary oxide system, it was necessary to create an ideal liquid solution phase from end-member liquid components $Na_2O_{(l)}$ and $Al_2O_{3(l)}$, and intermediates (associate species) $NaAlO_{2(l)}$ and $Na_2Al_4O_{7(l)}$:1/3. While the utility of including the $NaAlO_{2(l)}$ associate species is apparent from it existence in the system as a crystalline phase, the additional use of $Na_2Al_4O_{7(l)}$:1/3, which has no crystalline counterpart, was necessary in order to accurately reproduce the phase relations in the compositional region near Na_2O:Al_2O_3=1:2. The initial thermochemical values for the $NaAlO_{2(l)}$ species that are used when starting the phase diagram/thermodynamic data optimization were derived from the crystalline phase, whereas the $Na_2Al_4O_7$:$1/3_{(l)}$ species initial values were estimated.
This initial free energy of formation of the associate species, $NaAlO_{2(l)}$, is readily determined from considerations of the congruent melting reaction

$$NaAlO_{2(s)} = NaAlO_{2(l)} \qquad \Delta G = 0, \text{ at } T_{fusion} \qquad [1a]$$

where ΔG is the total free energy change for the reaction and T_{fusion} is the melting temperature. The 298 K heat of formation, $\Delta H_{f,298}$, for $NaAlO_{2(l)}$ is the 298 K heat of formation for $NaAlO_{2(s)}$ plus the heat of fusion, and the 298 K entropy of the solid is similarly adjusted to give the liquid species entropy by adding the entropy of fusion. The result is that at T_{fusion}

$$\Delta G_f(NaAlO_{2(s)}) = \Delta G_f°(NaAlO_{2(s)}) = Y_{Na2O}\Delta G_f(Na_2O_{(l)}) + Y_{NaAlO2}\Delta G_f(NaAlO_{2(l)}) + Y_{Na2Al4O7:1/3}\Delta G_f(Na_2Al_4O_7{:}1/3_{(l)}) + Y_{Al2O3}\Delta G_f(Al_2O_{3(l)}) \quad [1b]$$

where ΔG_f is the free energy of formation, $\Delta G_f°$ is the standard free energy of formation, and Y_i is the mole fraction of the liquid species i. The free energy and standard free energy of formation of the solid are identical since the pure stoichiometric solid phase is defined as having unit activity, a=1. The same may not be true for the liquid phase in equilibrium with this solid since the liquid solution is composed of $Na_2O_{(l)}$, $Al_2O_{3(l)}$, $NaAlO_{2(l)}$, and $Na_2Al_4O_{7(l)}$:1/3 liquid species with the constraint that the liquid composition be identical to that of the solid phase composition at the congruent melting temperature. Since the liquid solution is ideal, the following type of equation holds for each liquid species. $NaAlO_{2(l)}$ is used as an example, with Y_{NaAlO2} being the mole fraction (activity) of this species in the liquid solution.

$$\Delta G_f(NaAlO_{2(l)}) = \Delta G_f°(NaAlO_{2(l)}) + RT\ ln\ Y_{NaAlO2} \quad [1c]$$

Minimization of the total free energy determines the equilibrium state and the relative mole fractions of the species. Since the liquid phase is treated as an ideal solution, the activities of the liquid associate species are by definition equivalent to their mole fractions, $a_i = Y_i$, and these activities can be used to predict properties such as leaching behavior, corrosion reactions, and other important phenomena.

Chemical reactions and associated equilibrium constants can be used in determining the relative amounts of each species

$$Na_2O_{(l)} + Al_2O_{3(l)} = 2\ NaAlO_{2(l)} \qquad K_{eq} = \{Y_{NaAlO_2(l)}\}^2/\{Y_{Na_2O(l)}\ Y_{Al_2O_3(l)}\} \quad [2]$$

much as one would consider a homogeneous, equilibrium mixture of gaseous molecules. The activity values (mole fraction values) of these species at any given system composition could be inserted into equation [2] to calculate the value of K_{eq} at this temperature. Each system composition would result in the same value of K_{eq} at a given temperature for this reaction since for a given chemical reaction, K_{eq} is dependent only on temperature and not composition.

As noted above, equilibrium calculations that treat the end-member liquid species plus the associate species as an ideal solution allows complete description of the system. It is therefore possible to compute the phase relations and determine a phase diagram. ChemSage™ [14] was the primary tool for developing an assessed, internally consistent thermodynamic database, and for subsequent calculations of the equilibrium chemical behavior of the systems and drawing phase diagrams. The needed thermodynamic data are obtained from the literature, sources such as the assessed SGTE substance database, and estimates, and then simultaneously comparing and optimizing sets of phase equilibria and thermodynamic data.

Typically, the thermodynamic values for the associate species are not sufficiently refined as to allow accurate reproduction of the phase diagram. Melting and other transition temperatures are very sensitive to thermodynamic values, and therefore small differences can result in significantly skewed phase equilibria. Thus, the initial thermodynamic properties of the associate species are modified to calculate phase relations that match those of the experimentally

determined phase diagram. In the case of $NaAlO_{2(l)}$, as is often the general situation, the enthalpy of formation was slightly adjusted to fit the phase relations.

The chemical thermodynamic data set generated for the Na_2O-Al_2O_3 system allowed the final computed phase diagram to be drawn by ChemSage™, as depicted in Figure 1a. The diagram compares exceedingly well with the experimentally reported phase relations. The software also computes the individual activities of the species, and for the liquid/glass species these are plotted in Figure 1b for 800°C. The calculations were performed such that the crystalline phases in the system were allowed to exist, thus the non-varying activities are the result of two-phase regions where all degrees of freedom are fixed. In contrast, calculations constrained such that no crystalline phases form, as would be the case for an under-cooled liquid forming a glass, result in activities that vary smoothly (Figure 1c).

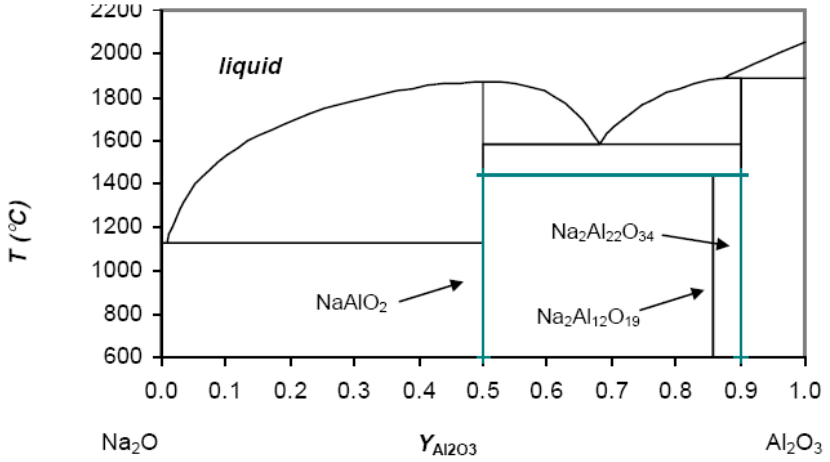

Figure 1a. Computed phase diagram for the Na_2O-Al_2O_3 system.

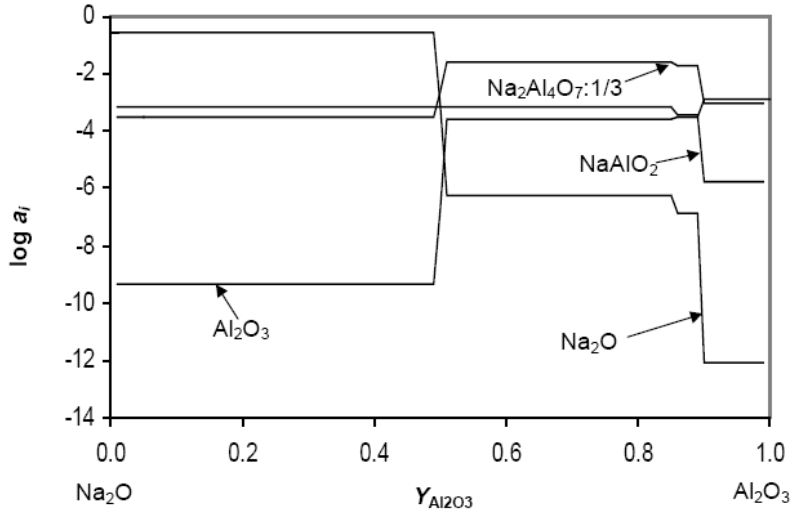

Figure 1b. Computed activities for the species in the associate species model for the glass phase in the Na_2O-Al_2O_3 system at 800°C where all crystalline phases are allowed to form. All lines should be horizontal or vertical as all degrees of freedom are fixed due to the presence of two phases over the entire compositional range.

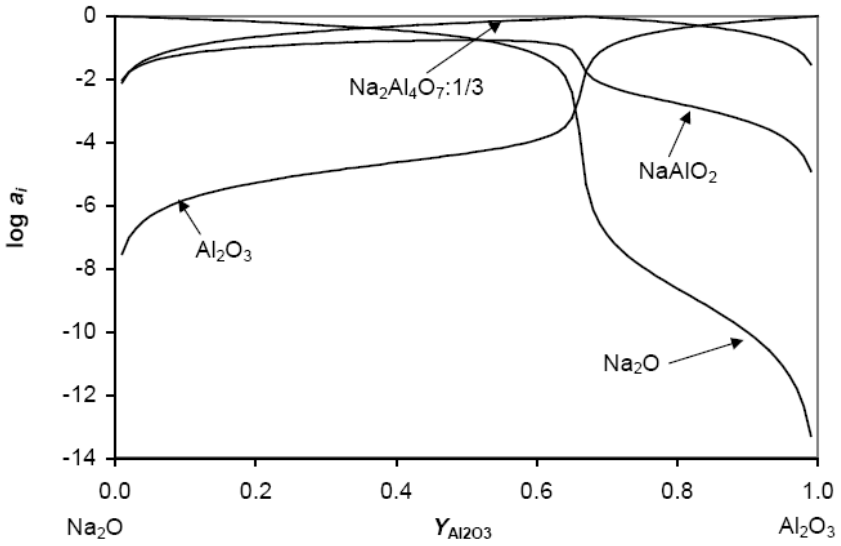

Figure 1c. Computed activities for the species in the associate species model for the glass phase in the Na_2O-Al_2O_3 system at 800°C where no crystalline phases are allowed to form. The curves vary continuously due to the presence of only the single glass phase.

The activities plotted in Figure 1c are illustrative of the relative stability, at least within the associate species model assumption, of the species in the glass. For this system the end member species, $Na_2O_{(l)}$ and $Al_2O_{3(l)}$, only have high activities near the terminal compositions, and therefore are not controlling chemical behavior over much of the compositional region. The most important species is the associate $Na_2Al_4O_{7(l)}$:1/3, which has a high activity over almost the entire compositional range, approaching unity at Na_2O:Al_2O_3 of 1:2, the species nominal composition that also coincides with the liquid eutectic composition between $NaAlO_2$ and $NaAl_9O_{14}$. As noted earlier, this indicates that the glass exhibits a high degree of interaction between the component oxides, and is thus not well-represented by an ideal mixture of the end-members.

8.4 CaO-SiO_2 System

The CaO-SiO_2 system is more complex to model and is a good example of treating liquid-liquid immiscibility using the modified associate species approach. As noted above, such immiscibility requires the solution to be treated as non-ideal, having positive interaction energies. The liquid for the CaO-SiO_2 system contains the end member species $Ca_2O_{2(l)}$ and $Si_2O_{4(l)}$ plus the associates $Ca_2SiO_{4(l)}$:2/3 (i.e., $Ca_{4/3}Si_{2/3}O_{8/3}$), $Ca_3SiO_{5(l)}$:1/2 (i.e., $Ca_{3/2}Si_{1/2}O_{5/2}$), and $CaSiO_{3(l)}$. Again, the unusual stoichiometries are required to maintain 2 non-oxygen gram-atoms per mol of each species.

Figure 2a contains the computed phase diagram for the CaO-SiO_2 system using parameters derived from the modified associate species model. The liquid-liquid immiscibility region required the inclusion of non-ideal interaction terms between $CaSiO_{3(l)}$ and $Si_2O_{4(l)}$ such that the excess free energy, G_{exs}, is:

$$G_{exs} = X(1-X)\ \{[141{,}000 - 65 \bullet T] + [(-10{,}000 - 10 \bullet T)(1-2X)]\} \qquad (3)$$

where T is the absolute temperature (K). Given the great sensitivities of phase equilibria to thermodynamic values, the phase diagram is well-reproduced with this model [18].

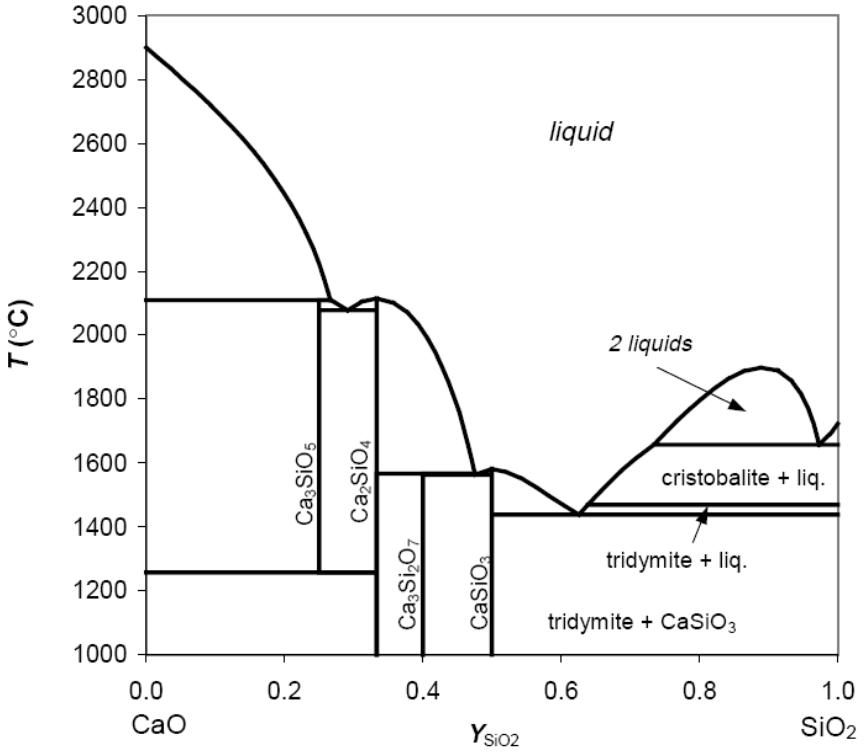

Figure 2a. Computed phase diagram for the CaO-SiO_2 system including representation of the two immiscible liquids region.

The chemical activities at 800°C of the species in the glass solution in the absence of crystalline phases were computed and are plotted in Fig. 2b. At high calcia contents the species $Ca_2O_{2(l)}$ and $Ca_3SiO_{5(l)}$:1/2 are dominant. In the high silica region the results of the positive interaction energies between $CaSiO_3$ and Si_2O_4 are apparent in their high activities, which approach unity. There are two glass phases present due to the immiscibility, thus constraining all the degrees of freedom and resulting in all activities being constant over this immiscible region.

8.5 Na_2O-Al_2O_3-B_2O_3-SiO_2 System

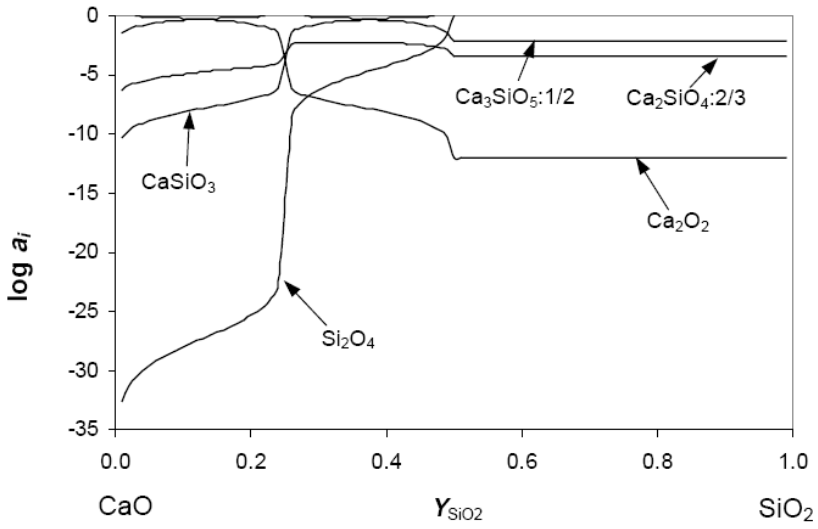

Figure 2b. Computed activities for the species in the associate species model for the glass phase in the CaO-SiO_2 system at 800°C where no crystalline phases are allowed to form. The curves vary continuously due to the presence of only the single glass phase at low silica content, but are invariant at high silica contents due to the presence of a second glass phase eliminating a degree of freedom.

In developing the thermodynamic data file for the quaternary Na_2O-Al_2O_3-B_2O_3-SiO_2 system, the thermodynamic and phase diagram data for six binary (Na_2O-Al_2O_3, Na_2O-B_2O_3, Na_2O-SiO_2, Al_2O_3-B_2O_3, Al_2O_3-SiO_2, and B_2O_3-SiO_2) and four ternary (Na_2O-Al_2O_3-B_2O_3, Na_2O-Al_2O_3-SiO_2, Na_2O-B_2O_3-SiO_2, and Al_2O_3-B_2O_3-SiO_2) subsystems were examined. In all cases, the complete set of thermochemical information for a system is refined and tested to give reasonable thermodynamic and phase diagram information over wide ranges of temperature and composition. Although a number of phases contain significant homogeneity ranges, in the current effort only mullite and nepheline were modeled as solid solutions over particular compositional ranges important to the proposed applications of the storage of nuclear waste in glass. Using the associate species approach for these crystalline solid solutions, successful models for the phases were developed. Nepheline was treated as an ideal solution of $NaAlSiO_4$, $NaAlSi_2O_6$, and $NaAlO_2$, and mullite was assumed to be composed of $Al_6B_{1.33}O_{11}$ and $Al_6Si_2O_{13}$. The phases and species contained in the data file are listed in Table I and an example of a computed pseudobinary phase diagram that accurately represents experimental observations is seen in Figure 3.

Table I. Phases and species in the Na_2O-Al_2O_3-B_2O_3-SiO_2 system that constitute the solutions utilizing the modified associate species model. The fixed composition crystalline phases in this system are also listed.

Glass	Solution Phases	Crystalline	
Na_2O	Mullite:	Na_2O	$Na_2B_8O_{13}$
Al_2O_3	$Al_6B_{1.33}O_{11}$	Al_2O_3	NaB_5O_8
B_2O_3	$Al_6Si_2O_{13}$	B_2O_3	NaB_9O_{14}
Si_2O_4		SiO_2 (cris)	Na_4SiO_4
$Al_6Si_2O_{13}$:/4		SiO_2 (trid)	$Na_6Si_2O_7$
$NaAlO_2$	Nepheline:	SiO_2 (quar)	Na_2SiO_3
$Na_2Al_4O_7$:/3	$NaAlSiO_2$	$NaAlO_2$	$Na_2Si_2O_5$
$Na_4B_2O_5$:/3	$NaAlSi_2O_6$	$Na_2Al_{12}O_{19}$	$Na_6Si_8O_{19}$
$NaBO_2$	$NaAlO_2$	$NaAl_9O_{14}$	$NaAlSi_3O_8$
$Na_2B_4O_7$:/3		Na_3BO_3	
$Na_2B_8O_{13}$:/5		$Na_4B_2O_5$	
Na_4SiO_4:2/5		$NaBO_2$	
Na_2SiO_3:2/3		$Na_2B_4O_7$	
$Na_2Si_2O_5$:/2		NaB_3O_5	
$NaAlSiO_4$:2/3			
$NaAlSi_2O_6$:1/2			

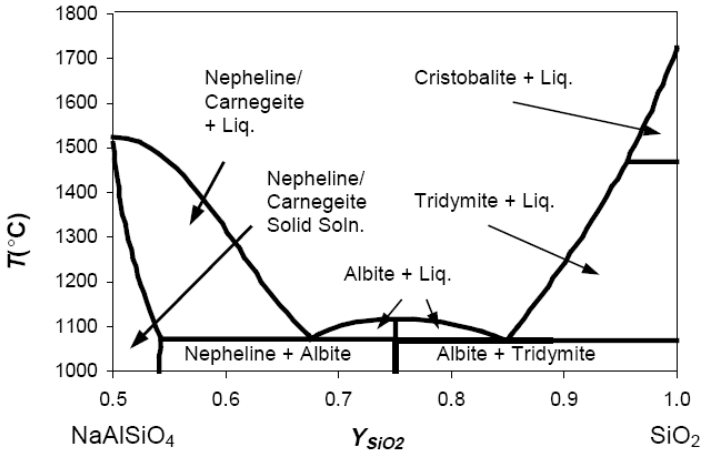

Figure 3 - Computed pseudobinary phase diagram over the compositional range from nepheline to silica.